The Plant Cell, Vol. 25: 5030–5042, December 2013, www.plantcell.org

Phosphatidic Acid Interacts with a MYB Transcription Factor and Regulates Its Nuclear Localization and Function in *Arabidopsis*[C][W]

Hongyan Yao,[a,b,c,d,1] Geliang Wang,[a,b,1] Liang Guo,[a,b] and Xuemin Wang[a,b,2]

[a] Department of Biology, University of Missouri, St. Louis, Missouri 63121
[b] Donald Danforth Plant Science Center, St. Louis, Missouri 63132
[c] School of Agriculture and Biology, Shanghai Jiaotong University, Shanghai 200240, China
[d] National Key Laboratory of Plant Molecular Genetics, Institute of Plant Physiology and Ecology, Chinese Academy of Sciences, Shanghai 200032, China

Phosphatidic acid (PA) has emerged as a class of cellular mediators involved in various cellular and physiological processes, but little is known about its mechanism of action. Here we show that PA interacts with WEREWOLF (WER), a R2R3 MYB transcription factor involved in root hair formation. The PA-interacting region is confined to the end of the R2 subdomain. The ablation of the PA binding motif has no effect on WER binding to DNA, but abolishes its nuclear localization and its function in regulating epidermal cell fate. Inhibition of PA production by phospholipase Dζ also suppresses WER's nuclear localization, root hair formation, and elongation. These results suggest a role for PA in promoting protein nuclear localization.

INTRODUCTION

Phosphatidic acid (PA) is a minor class of membrane lipids and a central intermediate in glycerolipid metabolism. PA was recently identified as a class of cellular messengers involved in a broad range of cellular and physiological processes in plants, animals, and fungi (Fang et al., 2001; Loewen et al., 2004; Mishra et al., 2006; Yang et al., 2008; Young et al., 2010). PA has been found to bind to various proteins, including transcription factors, kinases, phosphatases, enzymes involved in central metabolism, and proteins involved in vesicular trafficking and cytoskeletal rearrangements (Testerink et al., 2004; Zhang et al., 2004; Jang et al., 2012). It has been proposed that PA binding to proteins modulates the catalytic activity of target proteins, tethers proteins to the membrane, and promotes the formation and/or stability of protein complexes (Fang et al., 2001; Loewen et al., 2004; Nishikimi et al., 2009; Jang et al., 2012); however, little is known about the cellular effect of PA on its target proteins.

Polyphosphoinositides have been shown to modulate the intracellular localization and functions of various nuclear proteins (Manzoli et al., 1976; Fraschini et al., 1999; Hammond et al., 2004; Gonzales and Anderson, 2006). Phosphatidylinositol-4,5-bisphosphate [PtdIns(4,5)P_2] binds effector proteins to affect their nuclear localization, gene expression, RNA processing, mRNA export, and chromatin unfolding in animal cells (Yu et al., 1998; Zhao et al., 1998; Krylova et al., 2005; Mellman et al., 2008; Okada et al., 2008; Barlow et al., 2010). Phosphatidylinositol-5-bisphosphate [PtdIns(5)P] has been reported to promote protein translocation to the nucleus (Gozani et al., 2003) and also from the nucleus to the cytoplasm (Alvarez-Venegas et al., 2006; Viiri et al., 2009; Dieck et al., 2012). In yeast (*Saccharomyces cerevisiae*), PA in the endoplasmic reticulum (ER) binds to the transcriptional repressor OVERPRODUCER OF INOSITOL PROTEIN1 (Opi1p) and keeps it out of the nucleus, thus leading to the increase in the transcription of genes encoding phospholipid-metabolizing enzymes (Loewen et al., 2004). When the PA level at the ER membrane decreases, Opi1p translocates into the nucleus, where it inhibits a transcriptional activator complex and represses the expression of genes involved in phospholipid metabolism (Loewen et al., 2004). However, the effect of PA on promoting the nuclear translocation of proteins is unknown. Moreover, little is known about the role of phospholipid mediators in the localization and functions of nuclear proteins in plants.

In our screening of PA interactions with transcription factors potentially involved in lipid metabolism, the R2R3-type MYB (containing two repeats of a conserved myeloblastosis DNA binding domain of ~50 amino acids in length encoded by 3 α-helices) transcription factor WEREWOLF (WER) was identified as binding to PA. WER regulates GLABRA2 (GL2), a negative regulator of lipid production in *Arabidopsis thaliana* (Shen et al., 2006). In addition, WER is regarded as a master transcriptional regulator acting in nonhair cells to lead to nonhair cell fate through the downstream target GL2 (Di Cristina et al., 1996; Masucci et al., 1996; Lee and Schiefelbein, 1999; Ishida et al., 2007). On the other hand, a group of the R3-type MYB (containing one repeat of a conserved myeloblastosis DNA binding domain) proteins, CAPRICE (CPC), CAPRICE-LIKE MYB3 (CPL3), and ENHANCER OF TRY and CPC2 (ETC2), inhibit the action of WER, leading hair

[1] These authors contributed equally to this work.
[2] Address correspondence to swang@danforthcenter.org.
The author responsible for distribution of materials integral to the findings presented in this article in accordance with the policy described in the Instructions for Authors (www.plantcell.org) is: Xuemin Wang (swang@danforthcenter.org).
[C] Some figures in this article are displayed in color online but in black and white in the print edition.
[W] Online version contains Web-only data.
www.plantcell.org/cgi/doi/10.1105/tpc.113.120162

cells to initiate hair formation (Wada et al., 1997, 2002; Lee and Schiefelbein, 1999; Schellmann et al., 2002; Kirik et al., 2004a, 2004b; Ryu et al., 2005; Tominaga et al., 2007). In *Arabidopsis,* the root epidermal cells are generated at the root apical meristem and differentiate into two cell types, hair or nonhair cells (Dolan et al., 1994; Lee and Schiefelbein, 2002; Schiefelbein and Lee, 2006; Ishida et al., 2007; Kang et al., 2009). The cellular mechanisms by which these transcription factors are regulated are largely unknown.

The lipid mediator PA and its production enzyme phospholipase D (PLD) were recently implicated in both root hair formation and growth (Gardiner et al., 2003; Ohashi et al., 2003; Anthony et al., 2004; Li et al., 2006; Hong et al., 2009). PA has been found to bind 3-PHOSPHOINOSITIDE-DEPENDENT PROTEIN KINASE1 (PDK1) to promote root hair growth (Anthony et al., 2004). PLDε and its derived PA are involved in promoting root hair elongation (Hong et al., 2009). Inducible overexpression or suppression of *PLDζ1* increased or decreased root hair formation, respectively (Ohashi et al., 2003). However, knockout of *PLDζ1* affects root hair growth, but does not affect root hair patterning (Li et al., 2006), suggesting that the permanent loss of *PLDζ1* is compensated for by the other PLDs. In addition, suppression of PLD-mediated PA

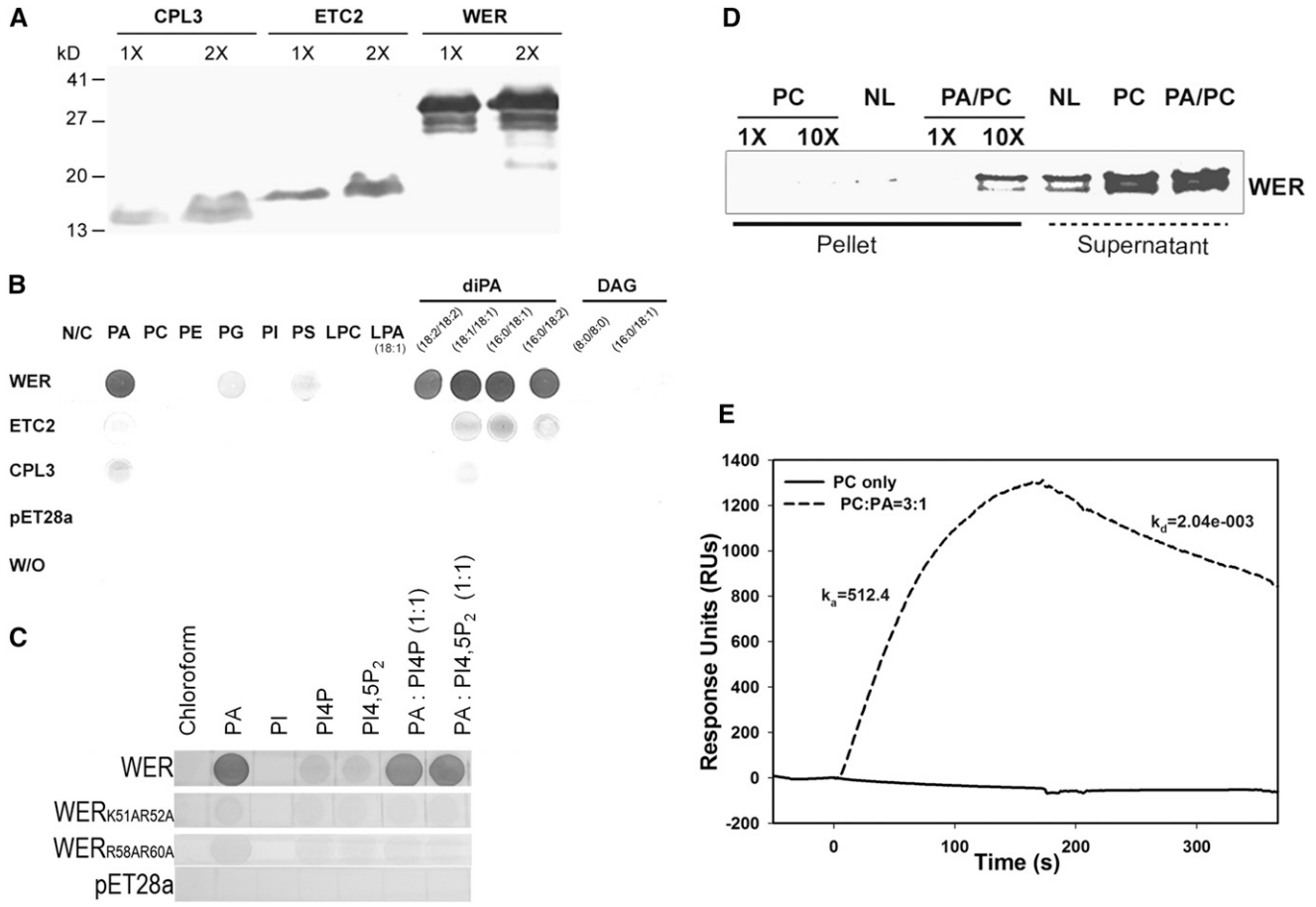

Figure 1. PA Binding to WER.

(A) Immunoblotting of His-WER, His-CPL3, and His-ETC2 expressed in *E. coli* Rosetta (DE3). Two concentrations of each protein were used for SDS-PAGE, followed by immunoblotting with anti-His-tag antibodies.

(B) Lipid-protein blotting of various lipids with WER, CPL3, or ETC2; 0.5 μg of each lipid was spotted on nitrocellulose strips. PA, PC, PE, PG, PI, PS, LysoPC, and LysoPA were from egg yolk, and the synthetic PA with defined acyl species was as specified.

(C) Lipid-protein blotting assay of PA, PI, PI4P, and $PI4,5P_2$ with WER and mutated WER; 0.5 μg of each lipid was spotted on nitrocellulose strips. PA and PI were from egg yolk, and PI4P and $PI4,5P_2$ were from porcine brain. Purified protein (WER and mutated WER, 0.5 μg/ml) was used, followed by immunoblotting with anti-His-tag antibodies.

(D) Liposomes were made up of di18:1-PC only or di18:1-PA/PC (1/3 mole ratio). 1× and 10× refer to the concentration gradient of PC or PA/PC liposomes used, with 10× indicating a 10 times higher concentration than 1×. NL, no liposome was used and only 25% of input WER used for liposomal binding was loaded.

(E) Representative SPR sensorgram of PA binding to WER. His-WER (2 μM) was immobilized on the NTA chip and 200 μM PC only or PA/PC (1/3 mole ratio) liposomes were injected. Each binding assay was repeated three times. Kinetic constants of PA binding to WER were calculated based on one sensorgram.

formation by primary alcohols alters root hair formation, morphology, and growth (Gardiner et al., 2003; Ohashi et al., 2003; Hong et al., 2009), implying the importance of PA in root hair development. However, how PA mediates root hair development is not understood. This study was undertaken to characterize the PA interaction with WER and the function of the lipid mediator binding in root hair growth and formation.

RESULTS

PA Interacts with WER

To study lipid interactions with transcription factors, we expressed and purified WER, CPL3, and ETC2, MYB transcription factors involved in regulating root hair formation (Figure 1A). We first tested the ability of these proteins to bind to various lipids using a lipid-protein blotting assay (Stevenson et al., 1998; Zhang et al., 2004). Using the same amount of proteins, WER gave strong PA binding signals on the blot, whereas CPL3 or ETC2 gave much weaker signals (Figure 1B). Dioleoyl PA displayed a strong binding signal, but other PA species tested also bound WER (Figure 1B). WER exhibited weak binding to phosphatidylglycerol (PG) or phosphatidylserine (PS), but no binding to other lipids, including phosphatidylcholine (PC), phosphatidylethanolamine (PE), phosphatidylinositol (PI), lysoPA, lysoPC, or diacylglycerol (DAG) (Figure 1B). WER did not display binding to polyphosphoinositides, including PtdIns(4)P or PtdIns(4,5)P_2, and the addition of PtdIns(4)P or PtdIns(4,5)P_2 to PA in a molar ratio of 1:1 also did not inhibit or enhance PA binding to WER (Figure 1C).

Liposomal binding was performed to verify the PA–WER interaction. The liposomes were made with either dioleoyl PC only or with a mixture of dioleoyl PC and dioleoyl PA in a molar ratio of 3:1. The mixture of PA with PC is needed because PA alone does not form a bilayer liposome. PA-containing liposomes bound to WER, and the amount of WER that was co-pulled down increased relative to the amount of liposomes (Figure 1D). By comparison, liposomes that contained only PC (referred to as PC-only liposomes) showed no binding (Figure 1D). The PA binding to WER was also demonstrated by surface plasmon resonance (SPR) (Figure 1E). In the representative sensorgram, response units (RUs) increased when the liposomes composed

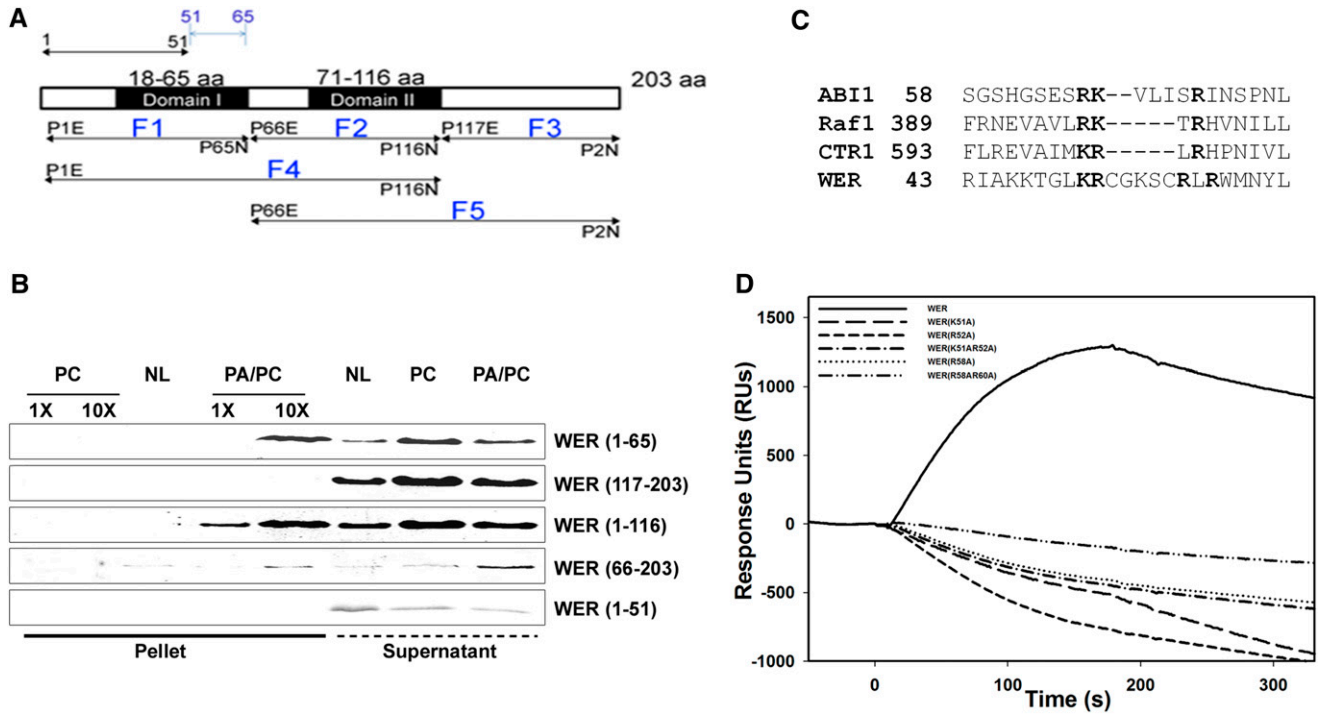

Figure 2. Identification of the PA Binding Motif and Amino Acid Residues Involved in WER Binding to PA.

(A) Schematic diagram showing serial deletions of WER. The WER fragments were expressed in *E. coli* and used for defining the PA binding domain.
(B) Binding of His-WER fragments to PA/PC liposomes. Liposomes were made up of di18:1-PC only or di18:1-PA/PC (1/3 mole ratio). 1× and 10× refer to the concentration gradient of PC or PA/PC liposomes used. NL, no liposome was used and only 25% of input WER fragment proteins used for liposomal binding was loaded.
(C) Sequence alignment of the PA binding fragment of WER with that of the PA binding motifs in chicken Raf1, abscisic acid insensitive 1 (ABI1), and constitutive triple response1 (CTR1) from *Arabidopsis*. The residues in bold are basic, potentially involved in PA binding and were mutated to Ala.
(D) Representative SPR sensorgram of PA binding to WER and its single and double mutants. Full-length His-WER or mutant WERs (2 μM) were immobilized on the NTA chip, followed by injection of PA/PC (1/3 mole ratio) liposomes.
[See online article for color version of this figure.]

of PA and PC bound to WER, whereas there was no increase in RUs when PC-only liposomes were injected, indicating that PA interacts specifically with WER (Figure 1E). Kinetic analysis for the interaction was determined by global fitting using BIA evaluation software. The PA–WER interaction has a low association rate constant, k_a = 512.4 $M^{-1}s^{-1}$, and an intermediate dissociation rate constant, $k_d = 2.04 \times 10^{-3}$ s^{-1}. The maximum specific binding was estimated to be 1823 RUs. The equilibrium binding constant K_D was calculated to be 3.99×10^{-6} M, indicating a high affinity between PA and WER.

The PA Binding Motif Resides in the R2 Subdomain

To identify the protein motif involved in PA binding, several deletion mutants of WER were constructed, taking into account the R2R3 domain structures (see Supplemental Figure 1 online). Five truncated polypeptides (Figure 2A) were produced in *Escherichia coli*, and binding was indicated by the detection of protein fragments in pellets of liposomes (Figure 2B). The N-terminal polypeptide of residues 1 to 65 (F1) displayed strong PA binding and residues 1 to 116 (F4) also exhibited binding (Figure 2B), whereas the C-terminal 117 to 203 (F3) fragment showed no PA binding (Figure 2B). Some F5 protein from residues 66 to 203 was recovered in the pellet, but similar amounts were also detected in fractions with no liposomes or PC-only liposomes, indicating nonspecific precipitation of F5 (Figure 2B). These results suggest that the PA binding domain resides within the first 65 amino acid residues (F1) in the R2 subdomain. To further define the segment of WER necessary for PA binding, we produced a deletion mutant of the N-terminal down to 51 amino acid residues. This mutant displayed no PA binding (Figure 2B). Thus, the PA binding to WER requires a short segment from amino acid residues 51 to 65 of WER.

No consensus sequence has been established for PA binding proteins, except for the PA binding domain in ABSCISIC ACID INSENSITIVE1, CONSTITUTIVE TRIPLE RESPONSE1, and Raf1, a polybasic KR/RK–R motif has been identified (Zhang et al., 2004; Wang et al., 2006; Testerink et al., 2007). The amino acid sequence of the PA binding 51 to 65 segment shows a low degree of similarity to the polybasic PA-interaction motif identified in plants and animals (Figure 2C). The R2 and R3 subdomains in WER each contain KR–R motifs (see Supplemental Figure 1 online), but the R3 polybasic motif is not involved in the PA binding. Therefore, we generated four mutants in the R2 subdomain with the basic amino acid residues substituted with Ala. SPR analyses of WER_{K51A}, WER_{R52A}, WER_{R58A}, $WER_{K51AR52A}$, and $WER_{R58AR60A}$ showed that mutated WERs had a greatly diminished ability to bind PA (Figure 2D). RUs of the mutated WER did not increase, whereas the full-length WER displayed a large RU increase and strong PA binding, as shown previously (Figure 2D). The SPR result was consistent with that of the liposomal binding assay, with both results indicating that these residues are critical for the binding of WER to PA.

The PA Binding Motif Is Required for WER's Nuclear Localization

To determine the role of PA binding in WER functions in plants, we transformed the non-PA binding $WER_{K51AR52A}$, $WER_{R58AR60A}$, or native WER into wild-type and *wer* mutant *Arabidopsis* and determined the effect of PA binding on the subcellular localization of WER protein in plants (Figure 3). Native and mutated WER coding regions ($WER_{K51AR52A}$; $WER_{R58AR60A}$) were fused with the yellow fluorescent protein (YFP) reporter under the control of the 35S promoter or with the green fluorescent protein (GFP) reporter

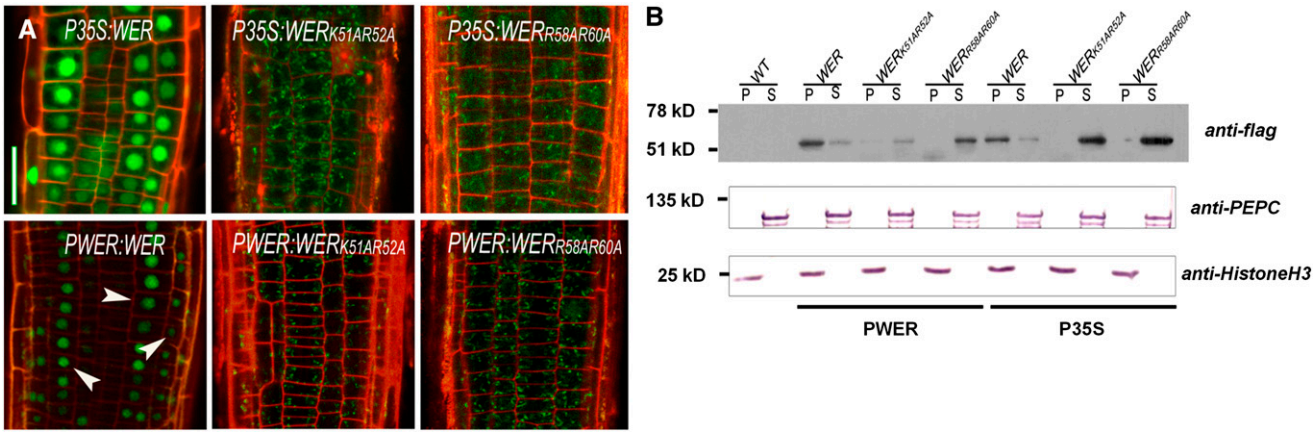

Figure 3. Subcellular Localization of WER, $WER_{K51AR52A}$, and $WER_{R58AR60A}$

(A) Longitudinal view (median section) of transgenic roots by confocal microscopy. *P35S:WER*, *P35S:*$WER_{K51AR52A}$, and *P35S:*$WER_{R58AR60A}$ were fused with YFP and *PWER:WER*, *PWER:*$WER_{K51AR52A}$, and *PWER:*$WER_{R58AR60A}$ were fused with GFP. The constructs were transformed into *Arabidopsis wer* mutants. GFP fluorescence in *PWER:WER wer* plants was mainly observed in the nucleus of the root epidermal cells (as marked by arrowheads). Roots were counterstained with propidium iodide to view cell boundaries. Bar = 100 μm.

(B) Immunoblotting of WER and mutant WER proteins expressed in *Arabidopsis*. P and S refer to proteins from nuclear pellets and soluble cytosol fractions, respectively. The same amounts of proteins (10 μg) were separated by SDS-PAGE and transferred onto a filter. WER proteins were detected using an anti-flag antibody conjugated with horseradish peroxidase. The proteins were immunoblotted with anti-PEPC and anti-histone H3 as cytosolic and nuclear markers, respectively. WT, wild type.

under the control of *WER* promoter. The WER-YFP/GFP fusion proteins are functional as demonstrated by their ability to genetically complement the *wer* mutant in root hair pattern formation. Transgenic plants in which the expression of the WER-YFP fusion was driven by the 35S promoter (*P35S:WER wer*) showed YFP fluorescence in the nuclei of all cells (Figure 3A; see Supplemental Figure 2 online). By contrast, the GFP fluorescence in *PWER:WER wer* plants occurred predominantly in the nucleus of the root epidermal cells, preferentially in the N-position cells and root tip cells (Figure 3A; see Supplemental Figure 2 online). The nuclear localization and the epidermal expression of *PWER:WER-GFP* are consistent with earlier observations (Lee and Schiefelbein, 1999; Ryu et al., 2005). By contrast, the mutated $WER_{K51AR52A}$ and $WER_{R58AR60A}$ were not detected clearly in the nucleus, regardless of the promoters used (Figure 3A).

To verify the results of subcellular distribution and also the level of WER proteins in the transgenic plants, the nuclear and cytosolic proteins from transgenic plants harboring WER or mutated WER were fractionated (Figure 3B). Phosphoenolpyruvate carboxylase 1 (PEPC1) and histone H3 were used as the cytosolic and nuclear markers, respectively, and the lack of PEPC1 in the nuclear pellet (P) and that of histone H3 in the cytosolic soluble (S) fraction suggest that the two fractions were well separated (Figure 3B). WER was detected in the nuclear and cytosolic fractions from the *P35S:WER* transgenic plants, but $WER_{K51AR52A}$ or $WER_{R58AR60A}$ was detected only in the cytosolic, and not the nuclear fractions (Figure 3B). To rule out that this change was not a result of overexpression, the same GFP fusion driven by the *WER* native promoter was examined. Again, WER-GFP was detected mostly in the nuclear fraction, whereas $WER_{K51A\ R52A}$-GFP or $WER_{R58AR60A}$-GFP was detected in the cytosolic fraction (Figure 3B).

Inhibition of PLDζs Also Renders WER in the Cytoplasm

To investigate whether PLD-produced PA is involved in the nuclear localization of WER, we used PLD inhibitors to suppress PA production, followed by examining the inhibitor effect on the nuclear localization of WER. The *Arabidopsis* genome has 12 PLD genes, but only PLDζ1 and PLDζ2 contain pleckstrin-homology (PH) and phox-homology (PX) domains, whereas the remaining 10 PLDs possess a C2 domain (Qin and Wang, 2002). The amino acid sequences of PLDζ1 and PLDζ2 are more similar to those of the mammalian PH/PX-containing PLD1 and PLD2 than to those of C2-containing PLDs in plants (Scott et al., 2009). Inhibitors specific to mammalian PLD1 and PLD2 were recently identified as (1*R*,2*R*)-*N*-

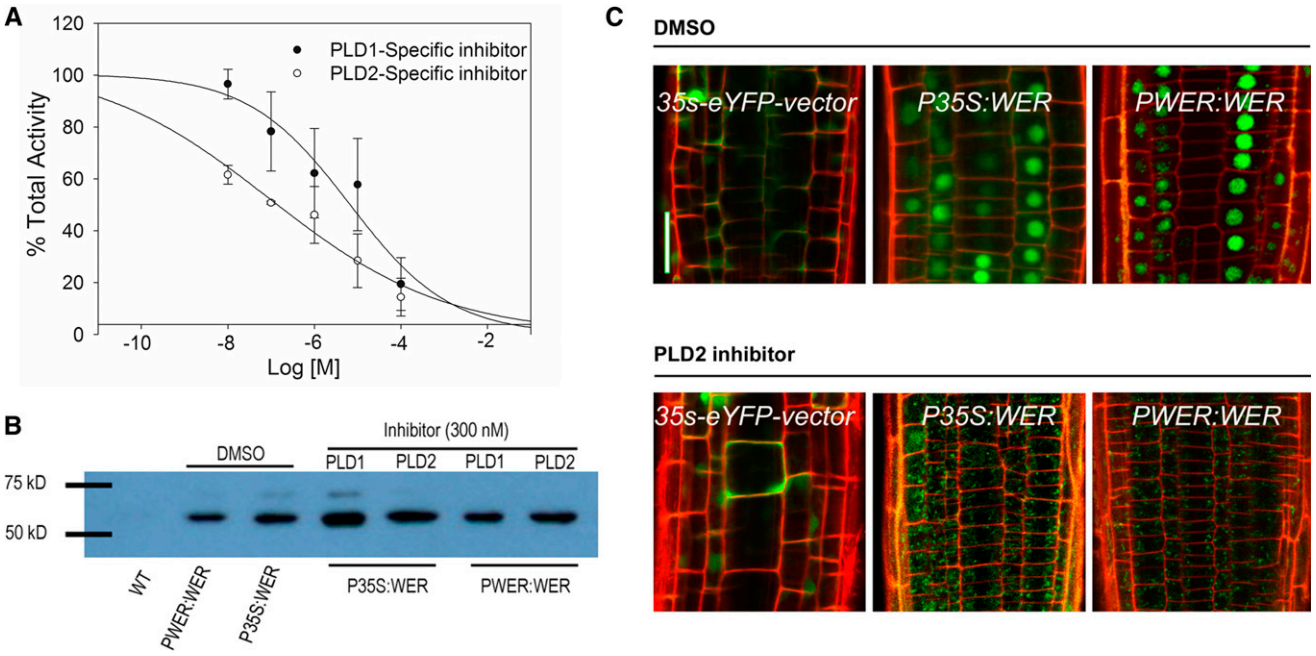

Figure 4. Inhibition of PLDζ Activity and Its Effect on Subcellular Association of WER.

(A) In vitro inhibition of PLDζ1 with PLD inhibitors, using *Arabidopsis* PLDζ1 produced in *E. coli*. The concentration response curves for each inhibitor are presented as a percentage of total PLD activity without inhibitor. Values are means ± SD (n = 3).

(B) Immunoblotting of WER expressed in *Arabidopsis*. Proteins (10 μg) extracted from roots were separated by SDS-PAGE and transferred onto a filter. WER was detected using an anti-flag antibody conjugated with horseradish peroxidase. WT, wild type.

(C) Longitudinal view (median section) of the root tip region of transgenic plants (transformed with *P35S:WER-YFP, PWER:WER-GFP*) treated with DMSO or PLD inhibitors (300 nM). YFP/GFP signals (green). Roots were counterstained with propidium iodide to view cell boundaries (red). Bar = 100 μm.

[See online article for color version of this figure.]

([*S*]-1-{4-[5-bromo-2-oxo-2,3-dihydro-1*H*-benzo[*d*]imidazol-1-yl] piperidin-1-yl}propan-2-yl)-2-phenylcyclopropanecar boxamide] and *N*-{2-[4-oxo-1-phenyl-1,3,8-triazaspiro(4.5)decan-8-yl]ethyl} quinoline-3-carboxamide, respectively (Scott et al., 2009). We explored the effectiveness of these inhibitors on plant PLDs, using the PH/PX-PLDζ1 and C2-PLDα1 that were expressed in *E. coli*. Both PLD1 and PLD2 inhibitors decreased the activity of PLDζ1 (Figure 4A), but displayed no inhibition on PLDα1 (see Supplemental Figure 3 online). The half-maximal inhibitory concentration (IC_{50}) for the PLD2 inhibitor is ~10 times lower than that for the PLD1 inhibitor (Figure 4A). Thus, the PLD2 inhibitor is more effective in inhibiting PLDζ1 activity than the PLD1 inhibitor. These differences are consistent with the amino acid sequence similarities between plant PLDζs and mammalian PLDs; PLDζ1 is more similar to mammalian PLD2 than to PLD1 (Qin and Wang, 2002). The PLD2 inhibitor requires the PX and PH domain for its inhibition (Scott et al., 2009), which may explain the lack of inhibition on the C2-containing PLDα1.

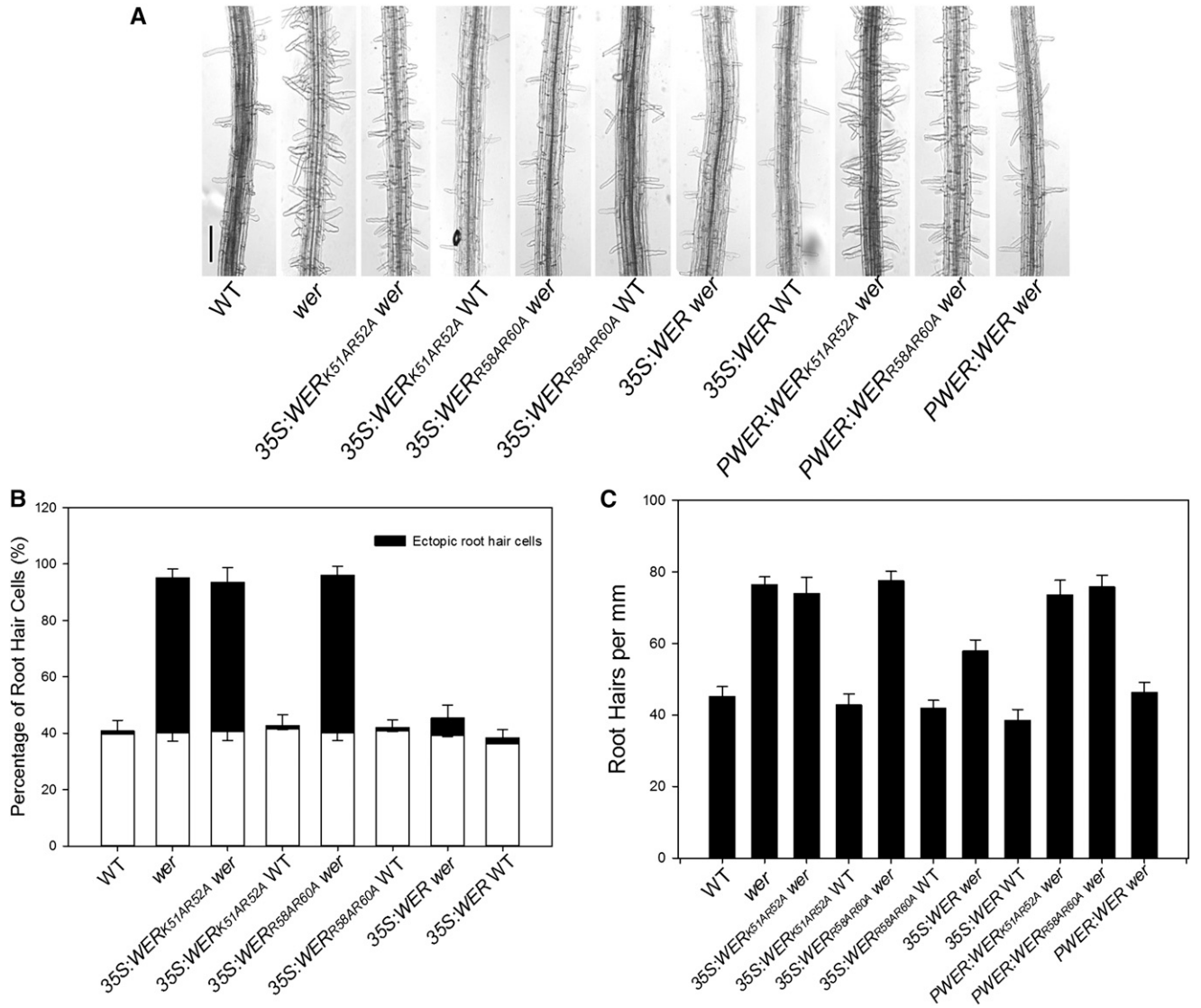

Figure 5. Root Hair Patterning as Affected by Transforming *WER* and Non-PA Binding Mutants to *Arabidopsis*.

(A) Root hair morphology of *WER-KO* (*wer*), wild type (WT), and both *wer* and wild-type plants harboring *P35S:WER*, *P35S:*$WER_{K51AR52A}$, *P35S:*$WER_{R58AR60A}$, *PWER:WER*, *PWER:*$WER_{K51AR52A}$, or *PWER:*$WER_{R58AR60A}$. Bar = 100 μm.

(B) Percentage of root epidermal cells that give rise to root hairs in wild-type, *wer*, and transgenic plants harboring WER or double mutants under the control of the 35S or WER native promoter.

(C) Root hair density of wild-type, *wer* and transgenic plants harboring *WER* or its double mutants under the control of the 35S or *WER* native promoter. Values are means ± SD (n = 5).

To investigate the effect of PLD inhibition on WER's subcellular association, we cultivated seedlings on Murashige and Skoog (MS) media with increasing levels of inhibitors. WER protein was produced in the inhibitor-treated seedlings, and thus the application of the inhibitor did not affect WER production (Figure 4B). In the *P35S:WER* seedlings, the WER-YFP signal was detected in almost all root epidermal cells. When they were cultivated on media with PLD2 inhibitors at 300 nM, only sporadic nuclear YFP signal was detected (Figure 4C). In *PWER:WER* roots, no GFP signal was observed in the nucleus when the PLD2 inhibitor concentration was above 300 nM.

Non-PA Binding WER Is Nonfunctional in Regulating Root Hair Patterning

To determine the function of the PA-WER interaction in root hair cell fates, we compared the number and pattern of root hairs in the roots of transgenic lines containing the non-PA binding $WER_{K51AR52A,}$ $WER_{R58AR60A}$, or native WER in wild-type and *wer* mutant *Arabidopsis* under the control of the 35S promoter or native *WER* promoter. Compared with the wild type, the *wer* mutant exhibited an increase in root hair cells with a decrease in hairless cells (Figure 5A). Almost all *wer* root epidermal cells (95 ± 3%) produced a root hair, regardless of their position, whereas 40% of wild-type root epidermal cells were hair cells (Figure 5B). This increase in root hairs was also shown when the root hair density was measured, which was ~90 hairs per millimeter for *wer* but only 45 hairs per millimeter for wild-type roots (Figure 5C).

When the *wer* mutant was complemented with *PWER:WER*, the root hair pattern and number were restored to those of wild-type *Arabidopsis* (Figure 5). When the *wer* mutant was transformed with *P35S:WER*, the portion of hair cells decreased to 45% (Figures 5B and 5C). However, transformation of the non-PA–binding $WER_{K51AR52A}$ or $WER_{R58AR60A}$ into the *wer* mutant caused no change in the root hair number or patterning from that of *wer* (Figure 5). The lack of effect occurred with $WER_{K51AR52A}$ and $WER_{R58AR60A}$ under the control of the *35S* and *WER* native promoter (Figure 5). Thus, ablation of the PA binding motif abolishes the function of WER in regulating epidermal cell fate.

We then examined the effect of PLD1 and PLD2 inhibitors on root hair growth by transferring 3-d-old seedlings onto 1/10 MS media with increasing concentrations of PLD inhibitors. The PLD2 inhibitor decreased root hair formation at 100 nM in both the wild type and *wer* and reached maximal inhibition at 300 nM (Figure 6A). The PLD1 inhibitor reached maximal suppression of root hair formation at 1000 nM (see Supplemental Figures 4A and 4B online). The different effectiveness is consistent with the inhibition of PLDζ1 activity by the two inhibitors (Figure 4A). When *PLDζ1*-KO, *PLDζ2*-KO, and *PLDζ1ζ2*-double knockout (KO) seedlings were grown in the presence of the PLD2 inhibitor, root hair formation was inhibited in *PLDζ1*-KO and *PLDζ2*-KO to a similar extent as in the wild type (Figure 6B). However, *PLDζ1ζ2*-double KO seedlings displayed less sensitivity to the PLD2 inhibitor, with a twofold greater number of root hairs than the wild type or single KO seedlings (Figure 6B). In addition, PLD inhibitors reduced root hair elongation in a dose-dependent manner, and the PLD2 inhibitor was more effective than the PLD1

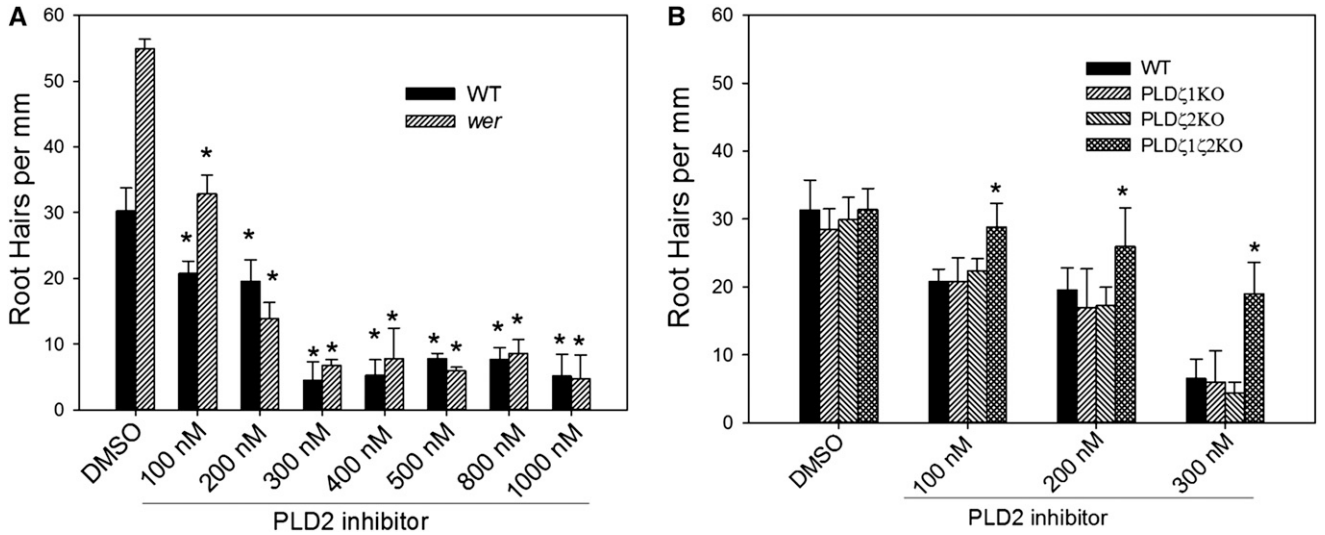

Figure 6. Effect of PLD2 Inhibitor on Decreasing Root Hair Density in Wild Type, *wer*, and *PLDζ*-KOs.

(**A**) Dose-dependence of PLD2 inhibitor on root hair density. *P < 0.05 difference from the corresponding genotype with DMSO treatment as assessed by the Student's *t* test.

(**B**) Root hair density of the wild type (WT), *PLDζ1*-KO, *PLDζ2*-KO, and *PLDζ1ζ2*-double KO, as affected by different concentrations of PLD2-inibitors *P<0.05 difference from the wild-type control under same treatment as assessed by the Student's *t* test. Values are means ± SD from root hairs of 10 seedlings.

inhibitor in reducing root hair elongation (see Supplemental Figures 4C and 4D online).

Non-PA Binding WER Is Still a Functional Protein

Because the binding site is in the R2 subdomain, we conducted a gel mobility shift assay using GL2MBS1 (Glabra2 MYB binding-sites 1) in the GL2 promoter as a probe to assess whether the mutations of PA binding amino acids affect the binding of WER to DNA. Incubation of WER or mutated WER proteins with GL2MBS1 all resulted in a shift of the digoxigenin-labeled DNA of GL2MBS1 and the shift was competitively abolished with the unlabeled GL2MBS1 DNA fragment (see Supplemental Figure 5 online). Thus, the mutated, non-PA binding WER still retains DNA binding abilities.

To test whether non-PA binding WER is a functional protein in plants, we fused a nuclear localization signal (NLS) to the C terminus of WER and non-PA binding WERs ($WER_{K51AR52A}$ and $WER_{R58AR60A}$) under the control of the *WER* native promoter, and transformed these constructs into *wer* mutant *Arabidopsis* (Figure 7A). The NLS fusion directed non-PA binding WERs ($WER_{K51AR52A}$ and $WER_{R58AR60A}$) to the nucleus, as indicated by the GFP signal in the root tip cells (Figure 7B). The localization of *PWER:GFP-*$WER_{K51AR52A}$*-NLS* and *PWER:GFP-*$WER_{R58AR60A}$*-NLS* WER was the same as that of *PWER:WER-NLS* (Figure 7B). The presence of *PWER:GFP-*$WER_{K51AR52A}$*-NLS* and *PWER:GFP-*$WER_{R58AR60A}$*-NLS* rescued the phenotype of the *wer* mutation, as did *PWER:WER-NLS,* as indicated by the decreased number of root hair density (Figure 7C). These results indicate that the non-PA binding mutations of WER affect WER's nuclear localization, but not its function.

DISCUSSION

Even though WER is found in the nucleus, it does not possess a detectable NLS based on its amino acid sequence (Ryu et al., 2005). This study indicates that PA binds to the MYB transcription factor WER and that the interaction is necessary for WER's nuclear localization. On the basis of our data from in vitro binding and nuclear association, as well as in planta non-complementation by the PA-nonbinding WER mutant and PLDζ inhibition, we propose that the PA interaction tethers WER to the nuclear membrane and this tethering is necessary for the localization of the proteins from the cytosol to the nucleus.

In yeast, PA in the ER was found to bind to the transcriptional repressor Opi1p, thereby keeping it out of the nucleus (Loewen et al., 2004). Thus, PA can promote or inhibit protein localization to the nucleus, depending on the specific protein. The different effects of PA are likely to be determined by the location and source of PA on the membranes, as well as other factors associated with the PA binding proteins. In the PA–Opi1p interaction,

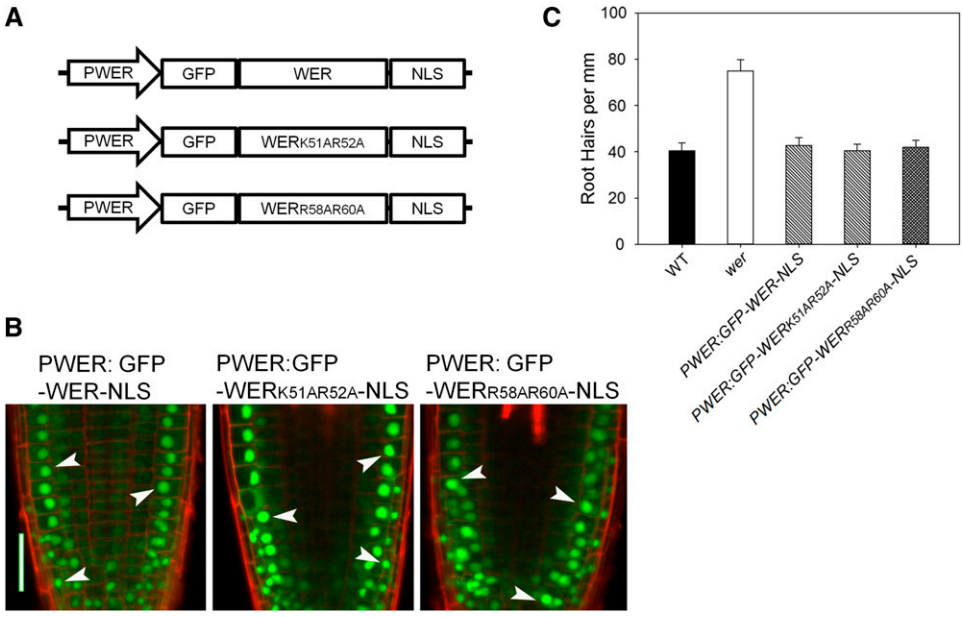

Figure 7. Subcellular Localization and Root Hair Patterning of an NLS-Fused GFP-WER-NLS, GFP-$WER_{K51AR52A}$-NLS, and GFP-$WER_{R58AR60A}$-NLS.

(A) Schematic illustration of the complementation constructs of WER and mutated WERs with a NLS fused at the C terminus and GFP fused at the N terminus under the control of WER native promoter (PWER).

(B) Longitudinal view (median section) of root tip region of *PWER:GFP-WER-NLS*, *PWER:GFP-*$WER_{K51AR52A}$*-NLS*, or *PWER:GFP-*$WER_{R58AR60A}$*-NLS* by confocal microscopy. The nuclear signal was found in epidermal cells and lateral root cap cells of all tested genotypes (as arrowheads). Bar = 100 μm.

(**C**) Root hair density of *wer* and transgenic complementation plants harboring *WER* or its double mutants fused with N-terminal GFP and C-terminal NLS. Values are means ± SD (n = 5).

[See online article for color version of this figure.]

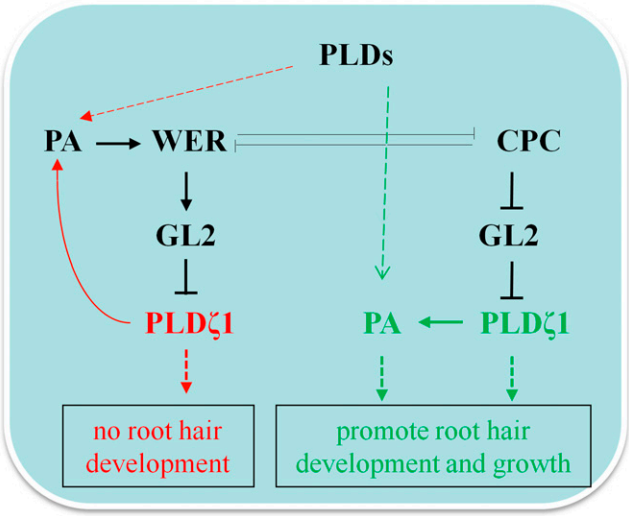

Figure 8. A Proposed Model Depicting the Role of the PA-WER Interaction in Feedback Attenuation of Root Hair Formation.

PA binding of WER acts as a feedback regulator to modulate root hair patterning. PLDs produce PA that binds to WER and promotes its nuclear localization, leading to the establishment of nonhair cells. In root hair cells, PLDζ1 catalyzes the formation of PA and promotes root hair formation and growth.
[See online article for color version of this figure.]

PA on the ER is metabolized for de novo lipid biosynthesis (Loewen et al., 2004), whereas in the PA–WER interaction, PLD contributes to the production of PA. The different routes of PA production regulate the spatial and temporal production of PA, as well as the molecular species of PA, which may result in the different effects of PA on the nuclear localization of its target proteins. Further studies on how PA helps promote the nuclear localization of a protein may reveal a mechanism for the nuclear translocation of proteins that lack a detectable NLS.

Similar to PA, phosphoinositides also have different effects on mediating protein nuclear localization via interaction with their target proteins (Manzoli et al., 1976; Fraschini et al., 1999; Hammond et al., 2004; Gonzales and Anderson, 2006; Viiri et al., 2012). PtdIns(5)P promotes the nuclear translocation of inhibitor of growth protein2, a candidate tumor suppressor protein, through binding to zinc fingers in the plant homeodomain of inhibitor of growth protein2 (Gozani et al., 2003). On the other hand, in *Arabidopsis*, PtdIns(5)P promotes translocation of antioxidant protein1, a histone 3 Lys4 trimethyltransferase, from the nucleus to the cytoplasm (Alvarez-Venegas et al., 2006). PtdIns(4,5)P_2 is a regulator of protein–protein and protein–nucleic acid interactions (Yu et al., 1998; Zhao et al., 1998; Krylova et al., 2005; Mellman et al., 2008; Okada et al., 2008; Barlow et al., 2010). In addition, PtdIns(4,5)P_2 is also an activator of PLDζ that produces PA (Testerink et al., 2007). These results show that PtdIns(4,5)P_2 does not bind to WER, and thus PLD may link PtdIns(4,5)P_2 and the PA-mediated regulation of nuclear processes.

Root hairs provide a large surface area through which plants take up water and nutrients. The formation and growth of root hairs are under complex control mechanisms, mediated by numerous factors. The results of our study suggest that the PA–WER interaction promotes both root hair formation and elongation (Figure 8). Multiple lines of evidence suggest a positive role for PLD and PA in root hair growth. Knockout of *PLDζ1* and *PLDζ2* reduces root hair growth under phosphate deprivation (Li et al., 2006), whereas *PLDε* promotes root hair elongation particularly under severe nitrogen limitation (Hong et al., 2009). We propose that PA binding of WER acts as a feedback regulator to modulate root hair patterning (Figure 8). A higher level of *PLDζ1* expression was detected in hair cells than in nonhair cells (Ohashi et al., 2003). PLD activity produces PA that binds to WER and promotes its nuclear localization. The nucleus-localized WER promotes the production of GL2, which binds to the promoter of *PLDζ1* and attenuates *PLDζ1* expression (Ohashi et al., 2003). These PA→WER→GL2→PLDζ1 interactions may lead to the establishment of nonhair cells. After cell fate differentiation, other PLDs may produce PA and PLDζ*1* may also still be active, to a small extent, in nonhair cells, together generating PA that binds to WER (Figure 8). On the other hand, in root hair cells, CPC suppresses WER function, and also the position-specific expression of *GL2* (Schiefelbein and Lee, 2006; Tominaga et al., 2007, 2008; Song et al., 2011). The CPC-mediated suppression of GL2 removes the GL2-mediated attenuation of *PLDζ1* expression, and thus PLDζ1 is active to produce PA and promotes root hair formation (Figure 8). The PA-WER interaction serves as part of the feedback loop that facilitates WER function, leading to attenuation of the PLD and PA functions (Figure 8).

An earlier study showed that the inducible overexpression or suppression of *PLDζ1* increased or decreased root hair formation, respectively (Ohashi et al., 2003). However, knockout of *PLDζ1* and *PLDζ2* did not affect root hair patterning (Li et al., 2006). In these analyses, chemical inhibition of *PLDζs* disrupted the nuclear localization of WER and root hair formation, but the gene knockout of both *PLDζ1* and *PLDζ2* did not alter root hair formation or WER's nuclear localization. These apparent discrepancies between inhibition and gene knockout results could mean that a genetic, permanent loss of *PLDζs* is compensated for by the presence of other PLDs and that the presence of PLDζ proteins impedes such compensation, as in the inhibitor-treated seedlings. The potential involvement of other PA-producing enzymes in the *PLDζ1ζ2*-double KO is consistent with the decreased sensitivity to the PLD2 inhibitor in the root hair formation that *PLDζ1ζ2*-double KO seedlings displayed over the wild type or *PLDζ*-single KO seedlings. One explanation for the lack of compensation in PLDζ-containing plants could be that besides PA production, PLDζ protein may be part of the regulatory complex that regulates root hair formation and growth (Figure 8). Thus, a less active, PLDζ-containing regulatory complex is attenuated in its ability to promote root hair growth. The PLDζ-like mammalian PLD1 and PLD2 have been reported to interact with more than 50 proteins, which include G proteins, protein kinases, and various structural proteins (Jang et al., 2012). Several proteins have also been found to interact with plant PLDα1, PLDβ, or PLDδ and the interactions are involved in different cellular processes (Mishra et al., 2006; Guo et al., 2012; Pleskot et al., 2013). It will be of great interest in future studies to determine the basis for the genetic compensation and the potential interaction of PLDζ with proteins involved in root hair growth and formation.

METHODS

Plant Materials

A *WER* T-DNA-insertional mutant *wer* in the *Arabidopsis thaliana* Columbia ecotype was identified from Salk_114008C, and seeds were obtained from the ABRC. To construct the overexpression vector, *WER* and mutated *WER* coding regions without a stop codon (*WER,* $WER_{K51AR52A}$, and $WER_{R58AR60A}$) were amplified using forward primer 5′-GCG TTAATTAA ATGAGAAAGAAAGTAAGTAG-3′ and reverse primer 5′-GCG GGTACC CAAAAACAGTGTCCATCTATAAAG-3′. These regions were then cloned into the pCAM-flag-EYFP vector. The *WER* open reading frame was fused with a flag tag at the N terminus and with eYFP at the C terminus. To construct the complementary vector, *WER* and mutated *WER* with a flag tag were amplified from the above vectors using the forward primer 5′-CGG CTGCAT ATGGACTACAAGGACGACGACGAC-3′ and the reverse primer 5′-CGG AGTACT GGTCGACTACTCGAGCTTCT-3′. The amplified fragments were digested with *Pst*I and *Sca*I and cloned into the pCBWERGFPN vector (between *Pst*I and blunted *Bam*HI restriction sites) with an mGFP5 fusion to the N terminus. To produce GFP-WER/mutated WER-NLS chimeric genes, *WER* and mutated *WER* were amplified using forward primer 5′-GCG CTGCAG ATGAGAAAGAAAGTAAGTAG-TAGTG-3′ and reverse primer 5′-GCG GGATCC TATCCTCCAACC-TTTCTCTTCTTCTTAGGAAGAAAACAGTGTCCATCTATA-3′, which includes the NLS sequence (underlined; Wolf et al., 2011). The amplified fragments were digested with *Pst*I and *Bam*HI and cloned into the pCBWERGRPN vector (between the *Pst*I and *Bam*HI restriction sites) encoding the GFP-WER/mutated WER-NLS. The binary vectors were then introduced into *Agrobacterium tumefaciens* strain GV3101 by a freezing and thawing method (Chen et al., 1994). The constructs were transformed into wild-type and *wer* plants using a floral dip method as previously reported (Clough and Bent, 1998). T1 seeds were harvested and transgenic plants were screened using 50 μM Basta for pCBWERGFPN constructs and 50 mg/L hygromycin for the pCAM-flag-eYFP vector. Seeds of wild-type, *wer*, and various transgenic plants were sown in soil and kept at 4°C for 2 d. Plants were grown in a growth chamber at 23°C with light/dark cycles of 16/8 h.

Construction of *WER* and its Mutants, and Protein Production in *Escherichia coli*

The cDNA-coding regions for the full-length and six deletion mutants of *WER* were amplified by PCR using the *WER* cDNA-coding region as a template and primers engineered to contain 5′-*EcoR*I and 3′-*Not*I restriction sites. All the cloning primer sequences are listed in Supplemental Table 1. An N-terminal common forward primer was paired with the four reverse primers to clone full-length $WER_{1–203}$ and the three deletion fragments $WER_{1–65}$, $WER_{1–116}$, and $WER_{1–51}$. A C-terminal reverse primer was paired with two forward primers to clone two other deletion fragments, $WER_{117–203}$ and $WER_{66–203}$. The $WER_{66–116}$ fragment was produced using primers listed in Supplemental Table 1. QuickChange site-directed mutagenesis (Stratagene) was used to generate the site-specific mutation from the full-length *WER* cDNA and mutated primers (see Supplemental Table 1 online) were used to generate WER_{K51A}, WER_{R52A}, WER_{R58A}, WER_{R60A}, $WER_{K51AR52A}$, and $WER_{R58AR60A}$. The cDNA-coding regions for full-length CPL3 and ETC2 were amplified by PCR using the respective cDNA-coding region as a template and engineered to contain 5′-*EcoR*I and 3′-*Not*I restriction sites using the specified primers (see Supplemental Table 1 online). All clones were confirmed to be error-free by DNA sequencing. These cDNAs were cloned into a pET28a expression vector fused with 6×His tag. The constructs were introduced into *E. coli* Rosetta (DE3) cells and expression was induced by treatment with 0.15 mM isopropyl-β-D-1-thiogalactopyranoside for 16 h at 16°C. The expressed protein was measured by immunoblotting with mouse monoclonal anti-polyHis antibodies conjugated with alkaline phosphatase. His-tagged WER and its mutated proteins were purified using Ni-nitrilotriacetic acid (NTA) agarose gel electrophoresis, according to the manufacturer's instructions (Qiagen).

Lipid-Protein Blotting and Liposomal Binding

PA-protein binding was first assayed using lipid-protein blotting according to the method of Stevenson et al. (1998), with minor modifications. Briefly, 0.5 μg of lipids dissolved in chloroform were spotted onto a nitrocellulose membrane and dried at room temperature. The membrane was preblotted in 3% (w/v) fatty acid–free BSA) in a mixture of Tris-buffered saline and Tween 20 (TBST;10 mM Tris-HCl, pH 8.0, 140 mM NaCl, and 0.1% Tween 20) for 1 h. The membrane was incubated for 12 h at 4°C with gentle shaking in the same solution containing WER, CPL3, or ETC2. After washing three times with TBST, the membrane was incubated with a rabbit anti-polyHis tag antibody (1:10,000; Sigma-Aldrich) for 1 h, followed by three washes with TBST. An anti-rabbit IgG conjugated with alkaline phosphatase (1:10,000; Sigma-Aldrich) was used as the secondary antibody. Binding of proteins to phospholipids was visualized by staining for alkaline phosphatase activity.

A liposomal binding assay was performed as previously described (Levine and Munro, 2002) with some modifications. Dioleoyl PC alone or mixed with dioleoyl PA in a molar ratio of 3:1 was dissolved in chloroform and dried under nitrogen. Lipids were rehydrated in 250 mM raffinose, 25 mM HEPES, pH 7.5, and 1 mM DTT for 1 h at 42°C, and then extruded repeatedly by a liposome extruder through a polycarbonate membrane (0.2-μm pore size), to produce an optically clear suspension of small unilamellar liposomes according to the manufacturer's instructions (Avanti). Liposomes were diluted with three volumes of binding buffer (25 mM HEPES, 125 mM KCl, 0.5 mM EDTA, pH 7.5, 1 mM DTT, 0.5 mM pheylmethylsulfonyl fluoride), harvested by centrifugation at 100,000*g* for 40 min, and resuspended in binding buffer to generate a stock with a final lipid concentration of 3.2 mM. For each protein binding assay, two concentrations of liposomes, 320 nmol and 32 nmol, were incubated with WER or mutant protein solution for 45 min at 25°C. The binding mixture with no liposome added was used as a negative control. Liposomes were pelleted at 14,000*g* for 30 min, washed twice with binding buffer, and pelleted again. The protein remaining in the supernatant was precipitated by the addition of 1/10 (v/v) of 100% trichloroacetic acid and washed twice with acetone and pelleted. Both liposome-bound proteins and proteins in the supernatants were detected by immunoblotting with mouse monoclonal anti-polyHis antibodies conjugated with alkaline phosphatase (1:10,000; Sigma-Aldrich).

SPR

SPR binding assays were performed using a Biacore 2000 system according to the manufacturer's instructions with some modifications. His-tagged WER and its mutant proteins were dialyzed in the running buffer overnight at 4°C, and then the protein concentration was measured. Biacore Sensor Chip NTA, which was designed to bind His-tagged proteins for interaction analyses, was used to immobilize the proteins. For each experiment, running buffer containing 500 μM $NiCl_2$ was injected to saturate the NTA with nickel. His-tagged WER proteins (2 μM) were immobilized on the sensor chip via Ni^{2+}-NTA chelation. Di18:1 PA/di18:1 PC liposomes (200 μM) from a 3.2 mM stock were resuspended in a running buffer (0.01 M HEPES, 0.15 M NaCl, 50 μM EDTA, pH 7.4) and injected in sequence over the surface of the sensor chip. The liposomes made with dioleoyl PC only were used as a control. For binding analysis of the point or double mutants of WER, 4 μM WER_{K51A}, WER_{R52A}, $WER_{K51AR52A}$, WER_{R58A}, or $WER_{R58AR60A}$ was immobilized on a sensor chip separately. Di18:1 PA/di18:1 PC liposome (200 μM) was injected in sequence to determine the interaction. The sensor chip was regenerated by stripping nickel from the surface with a regeneration buffer (0.01 M HEPES, 0.15 M NaCl, 0.35 M EDTA, pH 8.3). During the evaluation, the

sensorgrams from the beginning of association to the end of dissociation for each protein-liposome interaction were analyzed and plotted by SigmaPlot 10.0. Kinetic constants, including maximum specific binding (B_{max}), association rate constant (K_a), an intermediate dissociation rate constant (K_d), and the equilibrium binding constant (K_D), were analyzed using BIA evaluation software.

In Vitro PLD Activity Assays

PLDα1 and PLDζ1 were produced in *E. coli* and assayed as previously described (Pappan et al., 1997; Qin and Wang, 2002). Briefly, the PLDζ1 reaction mixture contained 100 mM Tris-HCl, pH 7.0, 80 mM KCl, 2 mM EGTA, and 2 mM EDTA, 0.4 mM lipid vesicles, and 30 μg of protein in a total volume of 200 μl. Lipid vesicles were composed of 35 nM PE, 3 nM PIP_2, and 2 nM PC containing dipalmitoylglycero-3-phospho-[methyl-^{3}H] choline as substrate. The PLDα1 assay mixture contained 100 mM MES, pH 6.0, 50 mM $CaCl_2$, 0.5 mM SDS, 0.4 mM lipid vesicles, and 30 μg of protein in a total volume of 200 μl. For both assays, the reaction was initiated by adding enzyme proteins, incubated at 30°C for 30 min in a shaking water bath, and stopped by adding 1 mL chloroform:methanol (2:1), followed by 100 μL 2 M KCl. The release of the [^{3}H]choline into the aqueous phase was quantified by scintillation counting.

PLD Inhibitor Treatment

The PLD1 (VU0359595) and PLD2 (VU0285655-1) inhibitors were purchased from Avanti Polar Lipids. The inhibitors were first dissolved in DMSO and diluted in solutions for PLD assays or growth media. To grow *Arabidopsis* on PLD inhibitor media, seeds of the wild type and *wer* mutants transformed with *PWER:WER-mGFP5*, *P35S:eYFP-WER* were germinated on 1/2 MS media with 0.6% agar for 3 d, and seedlings were then transferred onto 1/10 MS with 1.2% agar containing different concentrations of inhibitors. The seedlings were cultivated vertically in a growth chamber at 23°C with light/dark cycles of 12/12 h for 5 d. GFP or YFP expression was examined in roots stained with propidium iodide (10 μg/ml, 30 s) using a confocal laser scanning microscope (LSM-710; Carl Zeiss), with a 488 nm excitation mirror and a 505 to 530 nm and 530 to 560 nm emission filter to record images. To confirm WER expression, total proteins were extracted from roots and 10 μg protein was separated by 12% SDS-PAGE, followed by immunoblotting using an anti-flag antibody conjugated with horseradish peroxidase (1:2500). Seeds of *pldζ1* (Salk_083090), *pldζ2* (Salk_094369), and *pldζ1ζ2* (cross of Salk_083090 and Salk_094369) double mutants were also used to evaluate the effects of the inhibitors under the above-described conditions.

Root Hair Number

The number of root hairs was determined using a differential interference contrast microscope (Masucci et al., 1996) with some modifications. For each seedling root, five consecutive epidermal cells from the same cell file were observed, and a total of 20 cells from two hair cell files and the adjacent two nonhair cell files were counted. Any protrusion was scored as the presence of a root hair, regardless of the length.

Subcellular Localization of WER

The *wer* mutant was transformed with *PWER:WER-mGFP5*, *PWER:WER$_{K51AR52A}$-mGFP5*, *PWER:WER$_{R58AR60A}$-mGFP5*, *P35S:eYFP-WER*, *P35S:eYFP-WER$_{K51AR52A}$*, or *P35S:eYFP-WER$_{R58AR60A}$*. These plants were grown on agar-solidified media for 4 d. GFP or YFP expression was examined in seedlings stained with propidium iodide (10 μg/mL) using a confocal laser scanning microscope. For counterstaining with 4′,6-diamidino-2-phenylindole, dilactate (DAPI) (Sigma), the scans of YFP/GFP signals in roots were first examined under confocal microscopy, then roots were treated with 0.2% Triton X100 for 5 min, and sequentially dyed with 5 μg/ml DAPI for 2 min before examining the nuclear signals with the DAPI channel by confocal microscopy. To determine WER location by subcellular fractionation, proteins were extracted from roots of 4-week old transgenic plants using chilled buffer A (0.5 M Suc, 1 mM spermidine, 4 mM spermine, 10 mM EDTA, 10 mM Tris-HCl, pH 7.6, and 80 mM KCl), according to a previously reported method (Fan et al., 1999). The homogenate was filtered through miracloth and centrifuged at 3000*g* for 5 min. The nuclear pellet was gently dispersed in a suspension buffer (50 mM Tris-HCl, 5 mM $MgCl_2$, 10 mM β-mercaptoethanol, and 20% glycerol). The nuclear suspension was loaded onto a discontinuous Percoll gradient composed of 5 mL of 40%, 60%, 80% Percoll solution (0.44 M Suc, 25 mM Tris-HCl, pH 7.5, and 10 mM $MgCl_2$) on 5 mL 2 M Suc cushion. The gradients were centrifuged at 4000*g* in a swing-bucket rotor for 30 min. The supernatant from the gradient was analyzed as the cytosolic fraction, whereas the white nuclear band that appeared in the 80% Percoll layer above the 2 M Suc was removed with a Pasteur pipette. The nuclear fraction was washed twice by buffer A, pelleted by centrifugation at 6000*g*, and then resuspended in the nuclear resuspension buffer. For WER-flag detection, 10 μg of protein per lane was loaded and separated by 12% SDS-PAGE, followed by transfer onto a polyvinylidene difluoride filter. The filter was preblotted with phosphate buffered saline with tween 20 containing 5% BSA and then incubated with anti-flag antibodies (1:2500) overnight, followed by incubation with a polyclonal anti-rabbit IgG antibody conjugated with horseradish peroxidase (1:4000) for 2 h. The filter was washed three times with PBS containing 0.05% Tween 20, incubated with LumiGlo substrate for 1 min, and exposed to x-ray film. As a loading control, proteins from different fractions were separated on 8% SDS-PAGE gels and transferred onto a polyvinylidene difluoride filter. After blocking in PBS containing 5% nonfat milk, blots were probed with anti-PEPC (1:4000; Rockland) and anti-histone H3 (1:4000; Genscript) overnight at 4°C in blocking solution. Blots were washed three times for 15 min with TBST, followed by probing for 1 h with anti-rabbit IgG conjugated alkaline phosphatase secondary antibody in TBST (1:10,000). Finally, the blots were washed three times for 15 min in TBST, and then treated with Colorimetric AP substrate (Bio-Rad) for detection of protein bands.

Gel Mobility Shift Assay

DNA binding assays with WER and mutated WER proteins were performed as previously described (Koshino-Kimura et al., 2005) using a Roche DIG Gel Shift Kit (2nd Generation; Roche). Briefly, 100 ng of His-tagged WER or mutated WER proteins were incubated with 32 fmol of digoxigenin-labeled GL2MBS1 (5′TTCAACAACTCTTCTTTCCTGCCTTTACCGTTAGTCTAATTGTTTTCCTA-ATACTGCTAC-3′) oligonucleotide in 20 μL of binding buffer (10 mM Tris-HCl, pH 7.5, 50 mM NaCl, 1 mM EDTA, 10 mM DTT, 5% glycerol, 80 μg mL^{-1} poly (dI-dC) and 100 μg mL^{-1} BSA) at 22°C for 15 min. A 200-fold molar excess of unlabeled oligonucleotide was added as a specific competitor. The DNA–protein complexes were resolved on 0.75-mm thick 6% native polyacrylamide gels in 0.5× Tris-borate-EDTA buffer for 60 min at 8 V cm^{-1}.

Accession Numbers

Sequence data from this article can be found in the Arabidopsis Genome Initiative or GenBank/EMBL databases under the following accession numbers: wer (At5G14750), cpl3 (At4G01060), and etc2 (At2G30420); and *wer* (Salk_114008C), *pldζ1* (Salk_083090), *pldζ2* (Salk_094369), and *pldζ1ζ2* (cross of Salk_083090 and Salk_094369) double mutants.

Supplemental Data

The following materials are available in the online version of this article.

Supplemental Figure 1. The cDNA and Amino Acid Sequences of WER. The R2-DNA binding Domain I in WER Is Shown in Blue, and the R3-DNA Binding Domain II Is Shown in Green.

Supplemental Figure 2. The Expression Pattern and Nuclear Localization of *P35S:WER* and *PWER:WER* in *Arabidopsis* Root Tips.

Supplemental Figure 3. In Vitro Inhibition of PLDα1 with PLD Inhibitors.

Supplemental Figure 4. Effect of PLD1 and PLD2 Inhibitors on Root Hair Density and Length in the Wild Type and *wer*.

Supplemental Figure 5. Gel-Shift Assay for DNA Binding of WER and mutated WER.

Supplemental Table 1. PCR Primers Used for Cloning WER, Its Fragments, and Site-Specific Mutants, for cloning CPL3 and ETC2, and for Real-Time PCR.

ACKNOWLEDGMENTS

This research was primarily supported as part of the Center for Advanced Biofuels Systems, an Energy Frontier Research Center funded by the U.S. Department of Energy, Office of Science, Basic Energy Sciences under Award DE-SC0001295 and supported by the National Science Foundation under Award IOS-0818740 (inhibitor assays). H.Y. also acknowledges support from the Chinese Scholarship Council. The authors thank Myeong Min Lee for supplying pCBWERGFPN.

AUTHOR CONTRIBUTIONS

H.Y. cloned and expressed proteins, performed binding assays, and participated in article preparation. G.W. performed plant transformation, root hair analysis, subcellular localization, and PLD inhibitor assays, and participated in article preparation. L.G. helped with SPR analysis. X.W. directed the project and article preparation.

Received October 29, 2013; revised November 19, 2013; accepted December 3, 2013; published December 24, 2013.

REFERENCES

Alvarez-Venegas, R., Sadder, M., Hlavacka, A., Baluska, F., Xia, Y., Lu, G., Firsov, A., Sarath, G., Moriyama, H., Dubrovsky, J.G., and Avramova, Z. (2006). The *Arabidopsis* homolog of trithorax, ATX1, binds phosphatidylinositol 5-phosphate, and the two regulate a common set of target genes. Proc. Natl. Acad. Sci. USA **103:** 6049–6054.

Anthony, R.G., Henriques, R., Helfer, A., Mészáros, T., Rios, G., Testerink, C., Munnik, T., Deák, M., Koncz, C., and Bögre, L. (2004). A protein kinase target of a PDK1 signalling pathway is involved in root hair growth in *Arabidopsis.* EMBO J. **23:** 572–581.

Barlow, C.A., Laishram, R.S., and Anderson, R.A. (2010). Nuclear phosphoinositides: A signaling enigma wrapped in a compartmental conundrum. Trends Cell Biol. **20:** 25–35.

Chen, H., Nelson, R.S., and Sherwood, J.L. (1994). Enhanced recovery of transformants of *Agrobacterium tumefaciens* after freeze-thaw transformation and drug selection. Biotechniques **16:** 664–668, 670.

Di Cristina, M., Sessa, G., Dolan, L., Linstead, P., Baima, S., Ruberti, I., and Morelli, G. (1996). The *Arabidopsis* Athb-10 (GLABRA2) is an HD-Zip protein required for regulation of root hair development. Plant J. **10:** 393–402.

Dieck, C.B., Boss, W.F., and Perera, I.Y. (2012). A role for phosphoinositides in regulating plant nuclear functions. Front Plant Sci **3:** 50.

Clough, S.J., and Bent, A.F. (1998). Floral dip: A simplified method for *Agrobacterium*-mediated transformation of *Arabidopsis thaliana*. Plant J. **16:** 735–743.

Dolan, L., Duckett, C.M., Grierson, C., Linstead, P., Schneider, K., Lawson, E., Dean, C., Poethig, S., and Roberts, K. (1994). Clonal relationships and cell patterning in the root epidermis of *Arabidopsis.* Development **120:** 2465–2474.

Fan, L., Zheng, S., Cui, D., and Wang, X. (1999). Subcellular distribution and tissue expression of phospholipase Dα, Dβ, and Dγ in Arabidopsis. Plant Physiol. **119:** 1371–1378.

Fang, Y., Vilella-Bach, M., Bachmann, R., Flanigan, A., and Chen, J. (2001). Phosphatidic acid-mediated mitogenic activation of mTOR signaling. Science **294:** 1942–1945.

Fraschini, A., Biggiogera, M., Bottone, M.G., and Martin, T.E. (1999). Nuclear phospholipids in human lymphocytes activated by phytohemagglutinin. Eur. J. Cell Biol. **78:** 416–423.

Gardiner, J., Collings, D.A., Harper, J.D., and Marc, J. (2003). The effects of the phospholipase D-antagonist 1-butanol on seedling development and microtubule organisation in *Arabidopsis.* Plant Cell Physiol. **44:** 687–696.

Gonzales, M.L., and Anderson, R.A. (2006). Nuclear phosphoinositide kinases and inositol phospholipids. J. Cell. Biochem. **97:** 252–260.

Gozani, O., et al. (2003). The PHD finger of the chromatin-associated protein ING2 functions as a nuclear phosphoinositide receptor. Cell **114:** 99–111.

Guo, L., Devaiah, S.P., Narasimhan, R., Pan, X., Zhang, Y., Zhang, W., and Wang, X. (2012). Cytosolic glyceraldehyde-3-phosphate dehydrogenases interact with phospholipase Dδ to transduce hydrogen peroxide signals in the *Arabidopsis* response to stress. Plant Cell **24:** 2200–2212.

Hammond, G., Thomas, C.L., and Schiavo, G. (2004). Nuclear phosphoinositides and their functions. Curr. Top. Microbiol. Immunol. **282:** 177–206.

Hong, Y., Devaiah, S.P., Bahn, S.C., Thamasandra, B.N., Li, M., Welti, R., and Wang, X. (2009). Phospholipase D epsilon and phosphatidic acid enhance *Arabidopsis* nitrogen signaling and growth. Plant J. **58:** 376–387.

Ishida, T., Hattori, S., Sano, R., Inoue, K., Shirano, Y., Hayashi, H., Shibata, D., Sato, S., Kato, T., Tabata, S., Okada, K., and Wada, T. (2007). *Arabidopsis* TRANSPARENT TESTA GLABRA2 is directly regulated by R2R3 MYB transcription factors and is involved in regulation of GLABRA2 transcription in epidermal differentiation. Plant Cell **19:** 2531–2543.

Jang, J.H., Lee, C.S., Hwang, D., and Ryu, S.H. (2012). Understanding of the roles of phospholipase D and phosphatidic acid through their binding partners. Prog. Lipid Res. **51:** 71–81.

Kang, Y.H., Kirik, V., Hulskamp, M., Nam, K.H., Hagely, K., Lee, M.M., and Schiefelbein, J. (2009). The MYB23 gene provides a positive feedback loop for cell fate specification in the *Arabidopsis* root epidermis. Plant Cell **21:** 1080–1094.

Kirik, V., Simon, M., Huelskamp, M., and Schiefelbein, J. (2004a). The ENHANCER OF TRY AND CPC1 gene acts redundantly with TRIPTYCHON and CAPRICE in trichome and root hair cell patterning in *Arabidopsis.* Dev. Biol. **268:** 506–513.

Kirik, V., Simon, M., Wester, K., Schiefelbein, J., and Hulskamp, M. (2004b). ENHANCER of TRY and CPC 2 (ETC2) reveals redundancy in the region-specific control of trichome development of *Arabidopsis.* Plant Mol. Biol. **55:** 389–398.

Koshino-Kimura, Y., Wada, T., Tachibana, T., Tsugeki, R., Ishiguro, S., and Okada, K. (2005). Regulation of CAPRICE transcription by MYB proteins for root epidermis differentiation in *Arabidopsis.* Plant Cell Physiol. **46:** 817–826.

Krylova, I.N., et al. (2005). Structural analyses reveal phosphatidyl inositols as ligands for the NR5 orphan receptors SF-1 and LRH-1. Cell **120:** 343–355.

Lee, M.M., and Schiefelbein, J. (1999). WEREWOLF, a MYB-related protein in *Arabidopsis*, is a position-dependent regulator of epidermal cell patterning. Cell **99:** 473–483.

Lee, M.M., and Schiefelbein, J. (2002). Cell pattern in the *Arabidopsis* root epidermis determined by lateral inhibition with feedback. Plant Cell **14:** 611–618.

Levine, T.P., and Munro, S. (2002). Targeting of Golgi-specific pleckstrin homology domains involves both PtdIns 4-kinase-dependent and -independent components. Curr. Biol. **12:** 695–704.

Li, M., Qin, C., Welti, R., and Wang, X. (2006). Double knockouts of phospholipases Dzeta1 and Dzeta2 in Arabidopsis affect root elongation during phosphate-limited growth but do not affect root hair patterning. Plant Physiol. **140:** 761–770.

Loewen, C.J., Gaspar, M.L., Jesch, S.A., Delon, C., Ktistakis, N.T., Henry, S.A., and Levine, T.P. (2004). Phospholipid metabolism regulated by a transcription factor sensing phosphatidic acid. Science **304:** 1644–1647.

Manzoli, F.A., Cocco, L., Facchini, A., Casali, A.M., Maraldi, N.M., and Grossi, C.E. (1976). Phospholipids bound to acidic nuclear proteins in human B and T lymphocytes. Mol. Cell. Biochem. **12:** 67–71.

Masucci, J.D., Rerie, W.G., Foreman, D.R., Zhang, M., Galway, M.E., Marks, M.D., and Schiefelbein, J.W. (1996). The homeobox gene GLABRA2 is required for position-dependent cell differentiation in the root epidermis of *Arabidopsis thaliana*. Development **122:** 1253–1260.

Mellman, D.L., Gonzales, M.L., Song, C., Barlow, C.A., Wang, P., Kendziorski, C., and Anderson, R.A. (2008). A PtdIns4,5P2-regulated nuclear poly(A) polymerase controls expression of select mRNAs. Nature **451:** 1013–1017.

Mishra, G., Zhang, W., Deng, F., Zhao, J., and Wang, X. (2006). A bifurcating pathway directs abscisic acid effects on stomatal closure and opening in *Arabidopsis.* Science **312:** 264–266.

Nishikimi, A., et al. (2009). Sequential regulation of DOCK2 dynamics by two phospholipids during neutrophil chemotaxis. Science **324:** 384–387.

Ohashi, Y., Oka, A., Rodrigues-Pousada, R., Possenti, M., Ruberti, I., Morelli, G., and Aoyama, T. (2003). Modulation of phospholipid signaling by GLABRA2 in root-hair pattern formation. Science **300:** 1427–1430.

Okada, M., Jang, S.W., and Ye, K. (2008). Akt phosphorylation and nuclear phosphoinositide association mediate mRNA export and cell proliferation activities by ALY. Proc. Natl. Acad. Sci. USA **105:** 8649–8654.

Pappan, K., Zheng, S., and Wang, X. (1997). Identification and characterization of a novel plant phospholipase D that requires polyphosphoinositides and submicromolar calcium for activity in *Arabidopsis.* J. Biol. Chem. **272:** 7048–7054.

Pleskot, R., Li, J., Zárský, V., Potocký, M., and Staiger, C.J. (2013). Regulation of cytoskeletal dynamics by phospholipase D and phosphatidic acid. Trends Plant Sci. **18:** 496–504.

Qin, C., and Wang, X. (2002). The Arabidopsis phospholipase D family. Characterization of a calcium-independent and phosphatidylcholine-selective PLD zeta 1 with distinct regulatory domains. Plant Physiol. **128:** 1057–1068.

Ryu, K.H., Kang, Y.H., Park, Y.H., Hwang, I., Schiefelbein, J., and Lee, M.M. (2005). The WEREWOLF MYB protein directly regulates CAPRICE transcription during cell fate specification in the *Arabidopsis* root epidermis. Development **132:** 4765–4775.

Schellmann, S., Schnittger, A., Kirik, V., Wada, T., Okada, K., Beermann, A., Thumfahrt, J., Jürgens, G., and Hülskamp, M. (2002). TRIPTYCHON and CAPRICE mediate lateral inhibition during trichome and root hair patterning in *Arabidopsis.* EMBO J. **21:** 5036–5046.

Schiefelbein, J., and Lee, M.M. (2006). A novel regulatory circuit specifies cell fate in the *Arabidopsis* root epidermis. Physiol. Plant. **126:** 503–510.

Scott, S.A., Selvy, P.E., Buck, J.R., Cho, H.P., Criswell, T.L., Thomas, A.L., Armstrong, M.D., Arteaga, C.L., Lindsley, C.W., and Brown, H.A. (2009). Design of isoform-selective phospholipase D inhibitors that modulate cancer cell invasiveness. Nat. Chem. Biol. **5:** 108–117.

Shen, B., Sinkevicius, K.W., Selinger, D.A., and Tarczynski, M.C. (2006). The homeobox gene GLABRA2 affects seed oil content in *Arabidopsis.* Plant Mol. Biol. **60:** 377–387.

Song, S.K., Ryu, K.H., Kang, Y.H., Song, J.H., Cho, Y.H., Yoo, S.D., Schiefelbein, J., and Lee, M.M. (2011). Cell fate in the Arabidopsis root epidermis is determined by competition between WEREWOLF and CAPRICE. Plant Physiol. **157:** 1196–1208.

Stevenson, J.M., Perera, I.Y., and Boss, W.F. (1998). A phosphatidylinositol 4-kinase pleckstrin homology domain that binds phosphatidylinositol 4-monophosphate. J. Biol. Chem. **273:** 22761–22767.

Testerink, C., Dekker, H.L., Lim, Z.Y., Johns, M.K., Holmes, A.B., Koster, C.G., Ktistakis, N.T., and Munnik, T. (2004). Isolation and identification of phosphatidic acid targets from plants. Plant J. **39:** 527–536.

Testerink, C., Larsen, P.B., van der Does, D., van Himbergen, J.A., and Munnik, T. (2007). Phosphatidic acid binds to and inhibits the activity of *Arabidopsis* CTR1. J. Exp. Bot. **58:** 3905–3914.

Tominaga, R., Iwata, M., Okada, K., and Wada, T. (2007). Functional analysis of the epidermal-specific MYB genes CAPRICE and WEREWOLF in *Arabidopsis.* Plant Cell **19:** 2264–2277.

Tominaga, R., Iwata, M., Sano, R., Inoue, K., Okada, K., and Wada, T. (2008). *Arabidopsis* CAPRICE-LIKE MYB 3 (CPL3) controls endoreduplication and flowering development in addition to trichome and root hair formation. Development **135:** 1335–1345.

Viiri, K.M., Jänis, J., Siggers, T., Heinonen, T.Y., Valjakka, J., Bulyk, M.L., Mäki, M., and Lohi, O. (2009). DNA-binding and -bending activities of SAP30L and SAP30 are mediated by a zinc-dependent module and monophosphoinositides. Mol. Cell. Biol. **29:** 342–356.

Viiri, K., Mäki, M., and Lohi, O. (2012). Phosphoinositides as regulators of protein-chromatin interactions. Sci. Signal. **5:** pe19.

Wada, T., Kurata, T., Tominaga, R., Koshino-Kimura, Y., Tachibana, T., Goto, K., Marks, M.D., Shimura, Y., and Okada, K. (2002). Role of a positive regulator of root hair development, CAPRICE, in *Arabidopsis* root epidermal cell differentiation. Development **129:** 5409–5419.

Wada, T., Tachibana, T., Shimura, Y., and Okada, K. (1997). Epidermal cell differentiation in *Arabidopsis* determined by a Myb homolog, CPC. Science **277:** 1113–1116.

Wang, X., Devaiah, S.P., Zhang, W., and Welti, R. (2006). Signaling functions of phosphatidic acid. Prog. Lipid Res. **45:** 250–278.

Wolf, I., Kircher, S., Fejes, E., Kozma-Bognár, L., Schäfer, E., Nagy, F., and Adám, E. (2011). Light-regulated nuclear import and degradation of *Arabidopsis* phytochrome-A N-terminal fragments. Plant Cell Physiol. **52:** 361–372.

Yang, J.S., et al. (2008). A role for phosphatidic acid in COPI vesicle fission yields insights into Golgi maintenance. Nat. Cell Biol. **10:** 1146–1153.

Young, B.P., Shin, J.J.H., Orij, R., Chao, J.T., Li, S.C., Guan, X.L., Khong, A., Jan, E., Wenk, M.R., Prinz, W.A., Smits, G.J., and Loewen, C.J. (2010). Phosphatidic acid is a pH biosensor that links membrane biogenesis to metabolism. Science **329:** 1085–1088.

Yu, H., Fukami, K., Watanabe, Y., Ozaki, C., and Takenawa, T. (1998). Phosphatidylinositol 4,5-bisphosphate reverses the inhibition of RNA transcription caused by histone H1. Eur. J. Biochem. **251:** 281–287.

Zhang, W., Qin, C., Zhao, J., and Wang, X. (2004). Phospholipase D alpha 1-derived phosphatidic acid interacts with ABI1 phosphatase 2C and regulates abscisic acid signaling. Proc. Natl. Acad. Sci. USA **101:** 9508–9513.

Zhao, K., Wang, W., Rando, O.J., Xue, Y., Swiderek, K., Kuo, A., and Crabtree, G.R. (1998). Rapid and phosphoinositol-dependent binding of the SWI/SNF-like BAF complex to chromatin after T lymphocyte receptor signaling. Cell **95:** 625–636.